Asian Journal of Chemistry; Vol. 36, No. 9 (2024), 2089-2096

ASIAN JOURNAL OF CHEMISTRY

https://doi.org/10.14233/ajchem.2024.32202

Green Synthesis of Gold Nanoparticles using Neem Fruit Pulp Extract and their Applications in Catalytic and Antioxidant Activities

PIDAMARTHI SRAVANTHI[1,2], ALAMPALLY BANGARU BABU[1,3] and P.V. ANANTHA LAKSHMI[1,*]

[1]Department of Chemistry, Osmania University, Hyderabad-500007, India
[2]Telangana Tribal Welfare Residential Degree College (Boys), Maripeda, Mahabubabad-506315, India
[3]Department of Chemistry, Silver Jubilee Government College, Cluster University, Kurnool-517583, India

*Corresponding author: E-mail: pvanantha.ou@gmail.com

Received: 29 June 2024; *Accepted*: 23 July 2024; *Published online*: 30 August 2024; AJC-21735

Gold nanoparticles (AuNPs) were synthesized using an eco-friendly method involving *Azadirachta indica* (neem) fruit pulp extract. The characterization of the synthesized AuNPs were confirmed through UV–visible spectroscopy, FT-IR, DLS, XRD, EDX, AFM and HR-TEM techniques. The appearance of a dark brown colour visually indicated the formation of AuNPs, which was supported by a UV-visible absorbance peak around 455 nm. HR-TEM analysis revealed that the nanoparticles were spherical and averaged 20 nm in size. The synthesized AuNPs demonstrated significant antioxidant activity against DPPH. Additionally, they exhibited exceptional catalytic performance in the reduction of 4-nitrophenol and methylene blue dye when used with sodium borohydride. These findings suggest that the formation and applications of AuNPs could be valuable for advancements in pharmaceuticals and nanotechnology.

Keywords: Neem fruit pulp, Green synthesis, Gold nanoparticles, Catalytic reduction, Antioxidant activity.

INTRODUCTION

In recent years, the study of inorganic nanoparticles has expanded significantly due to their numerous practical applications in science and technology [1]. The unique catalytic, electrical, optical, magnetic and other physical and chemical properties of nanoparticles, which differ markedly from their bulk counterparts, are influenced by their size, shape and chemical environment, necessitating careful preparation [2,3]. Noble metal nanoparticles such as silver, gold, platinum, palladium and non-metallic inorganic oxides like zinc oxide and titanium oxide have been extensively utilized due to their distinct electronic, mechanical, optical, chemical and magnetic properties [4-9]. These nanoparticles possess unique characteristics such as a larger surface area to volume ratio, varied sizes and shapes (like spherical or rod-shaped) [10]. As a result, they find applications in diverse fields including diagnostic biological probes, optoelectronics, display instruments, catalysis, fabrication of biological sensors, detection and monitoring of diseases such as cancer cells, drug discovery, identification of environmental toxic metals or reagents and therapeutic uses [11-16]. Chemical and physical reduction methods are indeed the most prevalent and widely adopted techniques for preparing nanoparticles [17]. Nevertheless, these methods involve the use of toxic chemicals and physical processes which are costly, demand significant energy consumption and result in the formation of nanoproducts that may pose health risks [18,19].

Gold nanoparticles (AuNPs) are extensively researched nanoparticles known for their distinctive physico-chemical properties and excellent chemical stability [20-22]. These attributes make them suitable for various applications such as catalysis, bio-labeling, diagnostics and drug delivery [5,23-26]. Recently, the biogenic synthesis of gold nanoparticles (AuNPs) has been synthesized using biomaterials such as plant extracts, bacteria, fungi, enzymes and biopolymers [20,21,27].

Using plants for the synthesis nanoparticles provides a reliable and simple approach that eliminate employing various production steps. Phytochemicals in plants, including proteins, amino acids, polysaccharides, polyphenols and organic acids, help to reduce the Au^{3+} to Au^{0} and catalyze the formation of AuNPs [5,28]. Numerous reports highlighted the use of plants for synthesizing gold nanoparticles. Plants like avocado seed,

Avaroha carambola, onion peel, citrus and *Piper longum* have been used to produce AuNPs through straightforward processes, exploring their potential biological applications [23,29-32].

In this research, we explored a sustainable method for synthesizing gold nanoparticles using neem fruit pulp extract to reduce Au^{3+} ions in a gold solution to Au^0. *Azadirachta indica*, commonly known as neem or Indian lilac, is a medicinal plant from the Maliaceae family. This study demonstrates the efficient and straightforward synthesis of AuNPs using neem fruit pulp extract. The resulting nanoparticles were characterized using UV-visible spectroscopy, XRD, FTIR, DLS, EDX, XRD and HR-TEM techniques. Additionally, the AuNPs were evaluated for their antioxidant and catalytic reducing abilities.

EXPERIMENTAL

Aqueous extract of neem fruit: Fresh ripened neem fruits were collected from the botanical garden, Osmania University, Hyderabad, India and peeled off the skin as shown in Fig. 1. Deionized water (100 mL) was added to 20 g of peeled neem fruits and mixed at room temperature for 10 min and filtered through Whatman no. 1 filter paper. The filtrate was used as neem fruit extract (NFPE) was stored at -4 ºC for further studies.

Fig. 1. Image of neem fruits

Synthesis of gold nanoparticles: A mixture containing 3 mL of 0.5 mM $HAuCl_4 \cdot 3H_2O$ and 8 mL of 0.5% extract solution was heated in a microwave oven for 180 s. The colour of the reaction mixture changed slowly from pale yellow to ruby red, which indicates the formation of AuNPs. The formation of AuNPs is further confirmed by UV-visible spectroscopy and labelled as neem fruit pulp extract mediated gold nanoparticles (NFPE-AuNPs).

Effect of concentration of aqueous extract: In a test tube, 1 mL of 1 mM $HAuCl_4 \cdot 3H_2O$ solution was added to 3 mL of 0.3 mM liquid extract. The resulting solution was heated in a microwave oven for 180 s. Same procedure was repeated for following concentrations of fruit extract 0.5, 0.8, 1, 1.25 and 1.5% and then measured the UV-vis spectra of each solution.

Effect of salt: In 50 mL beaker, 1 mL solution of 0.1 mM solution of $HAuCl_4 \cdot 3H_2O$ was mixed with 3 mL of fruit extract was added into it and then heated in a microwave for 180 s. The same procedure was repeated with different concentrations of $HAuCl_4$ having 0.2 mM, 0.3 mM, 0.4 mM, 0.5 mM and 0.6 mM. Finally, the UV-vis spectral analysis of each solution was analyzed.

Characterization: The UV-visible analyses were conducted in the range of 300 to 1000 nm using a Shimadzu UV-1800 UV-VIS spectrometer to monitor the reduction of NFPE-AuNPs. The average particle size in solution and zeta potential of synthesized AuNPs were measured with Horibia nanoparticle analyzer (SZ100) using dynamic light scattering (DLS) method. Following this, the gold nanoparticles were subjected to oven drying at 60 ºC for 1 day before being examined for structural and compositional analysis using powder X-ray diffraction Brucker D8 advanced twin-twin spectroscopic instrument operated at 45 kV and 20 mA with scanning occurring within the range of 2θ = 10-80º @ 2º/min. Transmission electron microscopy (TEM), utilizing a Jeol/JEM2100 instrument, was employed to investigate the size and morphology of AuNPs. Additionally, FTIR analysis was conducted with a Thermo-Scientific Nicolet 6700 system to identify the bioreduction compounds responsible for the reaction. Spectra were recorded within the range of 4000-550 cm^{-1}.

Catalytic reduction of 4-nitrophenol: The catalytic activity of NFPE-AuNPs was investigated using the reduction of 4-nitrophenol as model reaction. Initially, 4-nitrophenol (0.4 mM, 1 mL) was mixed with deionized water (1.8 mL) in a quartz cuvette followed by the addition of $NaBH_4$ (200 mM, 200 µL) solution. Subsequently, NFPE-AuNPs (100 µL) were introduced as a catalyst. The reaction progress was monitored using UV-visible spectrophotometer at different time intervals.

Catalytic reduction of methylene blue dye: The catalytic reduction activity of NFPE-AuNPs for reduction of methylene blue dye was studied using the UV-visible spectrophotometer with freshly prepared $NaBH_4$ solution at room temperature. In a quartz cuvette, 1.8 mL of methylene blue dye (0.05 mM) solution was taken along with 1 mL of freshly prepared $NaBH_4$ (10 mM). Then 100 µL of nanoparticles was added and the reduction reaction was monitored after the interval of 1 min using UV-visible spectroscopy.

DPPH radical scavenging activity: The antioxidant activity of NFPE-AuNPs against the DPPH radical were assessed by following Blois' method [33]. Different concentrations (25, 50, 75 and 100 µg/mL) of sample dissolved in 1 mL of DMSO were mixed with 4 mL of 0.004% (w/v) DPPH solution in methanol. After a 30 min incubation period at room temperature, the absorbance was measured at 517 nm against a blank. Ascorbic acid served as the standard for comparison. Each experiment was conducted in triplicate and the results were averaged. The inhibition percentage (I%) of DPPH radical formation was determined using the following equation:

$$\text{Inhibition (\%)} = \frac{A_{control} - A_{sample}}{A_{control}}$$

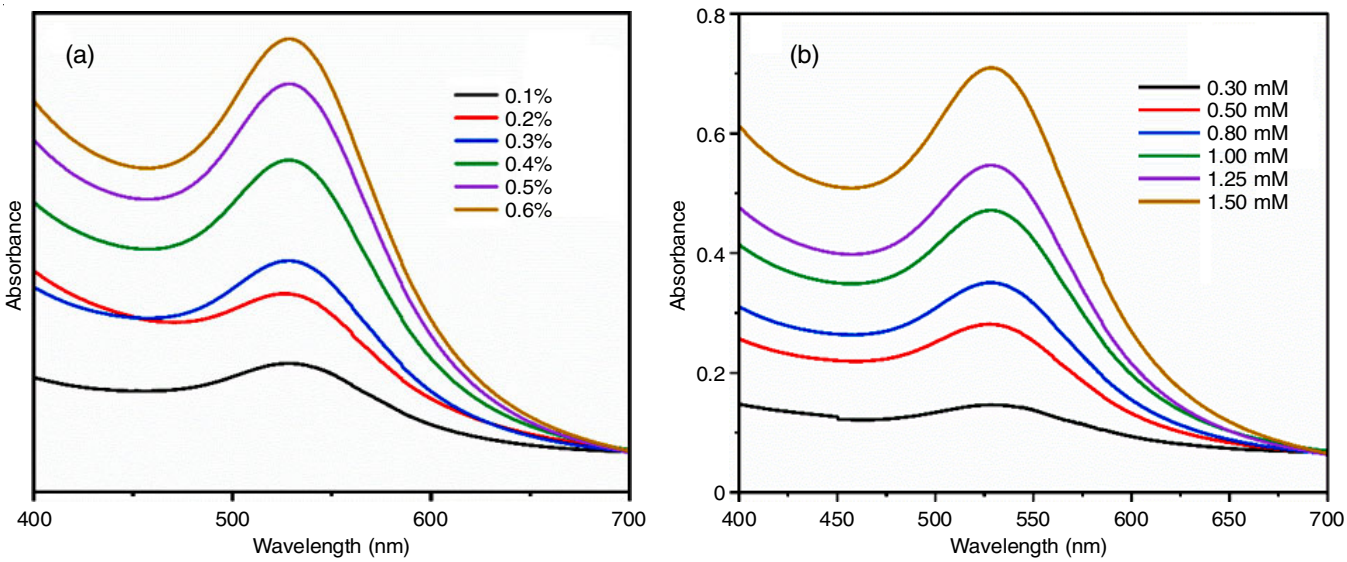

Fig. 2. UV-vis spectra of AuNPs showing the effect of (a) extract concentration and (b) gold salt concentration on the synthesis

RESULTS AND DISCUSSION

The neem fruit pulp extract (NFPE-AuNPs) was utilized to obtain gold nanoparticles by an approach mediated by a plant extract. The process began by adding an aqueous solution of NFPE to $HAuCl_4$. Aqueous gold solution is light yellow in colour and colour of liquid extract of neem fruit is colourless. Colour of gold solution remains unchanged as addition of liquid extract at first. When the mixed solution was kept in microwave colour changed into ruby red [30]. A peak at 529 nm appeared in its UV-visible spectra, which specified the formation of gold nanoparticles. This colour change is attributed to the surface plasmon resonance (SPR), which results from the collective oscillation of AuNPs electrons in resonance with light [34].

As shown in Fig. 2a, the reduction of Au^{3+} into Au^0 by NFPE and the formation of AuNPs was evidenced by the UV-vis spectra for all the NFPE concentrations. The effect of extract concentration on the synthesis of AuNPs was studied by UV-visible absorption spectra produced by the microwave irradiation of different concentrations of plant extract (0.1 to 0.6 %) with 1 mm of $HAuCl_4$ solution for 80 s (Fig. 2a). It was observed that the absorbance intensity of the reaction mixture increased with the increase in the concentration of plant extract indicating the higher production rate of nanoparticles. Gold nanoparticles synthesized with 0.1% NFPE showed low absorbance, likely due to an insufficient amount of reducing agents available to react with Au^{3+} ions in the solution and the reaction with 0.6% NFPE displayed a SPR band at 530 nm, suggesting the formation of larger and anisotropic AuNPs. A rapid colour change was noted in mixtures containing 0.5% and 0.6% NFPE, this is due to the higher concentration of reducing agents present in reaction mixture. Hence, 0.5% NFPE was chosen as the optimal concentration for AuNP synthesis.

The effect of $HAuCl_4$ concentration on the synthesis of AuNPs was studied by UV-visible technique at different concentration (0.1 to 0.6 mM) containing 0.5 % plant extract for 80 s of microwave irradiation (Fig. 2b). The obtained AuNPs with 0.3 and 0.5 mM $HAuCl_4$ exhibited broad SPR peaks with low absorbances indicated that AuNPs formation was not favourable at these concentrations. A sharp, narrow and symmetrical peak at 530 nm were observed at 0.8, 1.0 and 1.25 mM $HAuCl_4$. The results were in accordance with other studies, where the biosynthesis of nanoparticles increased with the increase in ion salt concentration. Therefore, 1 mM $HAuCl_4$ was chosen as the optimum salt concentration for the synthesis of AuNPs.

IR spectra: The FT-IR analysis indicated a wide variety of phytochemicals and functional groups on the AuNPs surface. FT-IR spectrum recognizes the functional groups of the phytochemicals that are the reason for the reduction of gold ions (Au^{3+}) ions to gold (Au^0) nanoparticles and subsequent stabilization of the AuNPs present in plant extract (Fig. 3). The FT-IR spectrum of neem fruit pulp extract exhibits strong vibrations at 3411 cm^{-1} (O-H an N-H stretching alcohols & amines), 1628 cm^{-1} (N-H bending), 1153 cm^{-1} (C-C skeletal vibrations) and

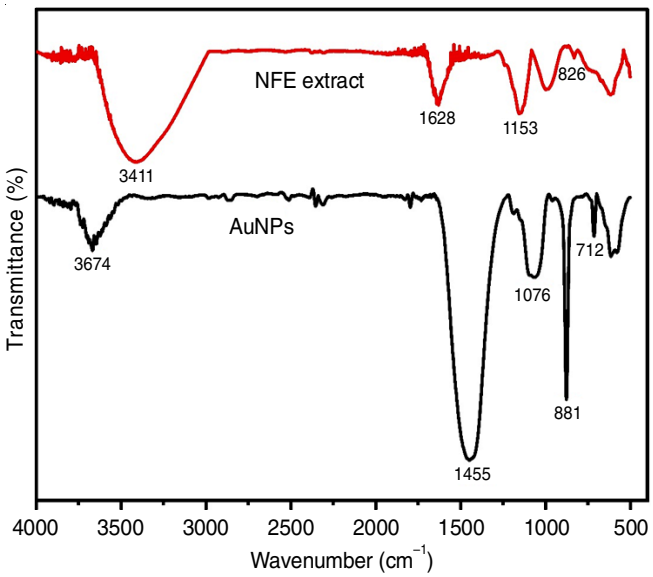

Fig. 3. Representative FT-IR spectra of NFE and AuNPs

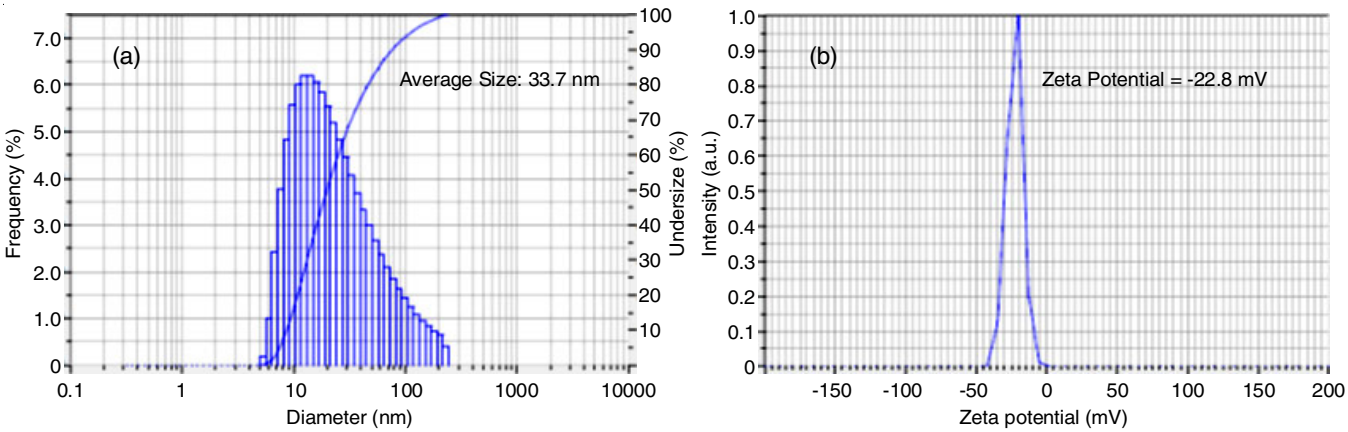

Fig. 4. (a) Size distribution histogram of AuNPs, (b) DLS for zeta potential of AuNPs

826 cm^{-1} (C-X stretching). The reduction of Au^{3+} to Au^0 results in a strong band at 3674 cm^{-1} (O-H and N-H stretching alcohols & amines), 1455 cm^{-1} (C-N stretching 2º amine) and 1076 cm^{-1} (C-O stretching alkyl ether), 881 and 712 cm^{-1} (C-X stretching). The presence of hydroxyl, amine and halo compounds in the extract of NFPE contains are responsible for the reduction and stability of NFPE-AuNPs. The similar results are already been reported [22,35, 36].

Particle size and zeta potential analysis (dynamic light scattering (DLS): The size distribution and zeta potential in colloidal solutions can be determined using dynamic light scattering (DLS). The average size of the AuNPS synthesized was found to be 33.7nm (Fig. 4a). The particles ranged from 10 nm to 100 nm in distribution. The Zeta potential of AuNPs measured at -22.8 mV (Fig. 4b) indicates a negative charge. These particles exhibit colloidal stability due to strong repulsions between them, preventing agglomeration.

EDX spectra: The conversion of Au^{3+} into Au^0 nanoparticles through bioreduction was confirmed using EDX analysis. Fig. 5 shows the EDX spectrum of the synthesized NFPE-AuNPs. The identification of elemental gold signals at different energy levels (2.2 keV, 8 keV, 9.75 keV, 11.5 keV and 13.4 keV). The prominent peaks of gold absorption observed at 2.2 keV are likely indicative of the gold binding energy [37]. Signals from other elements such as C, O, Cl and K were also observed, attributed to non-focal elements present in NFPE. Moreover, the presence of carbon, chlorine, potassium and oxygen peaks suggests the involvement of biological molecules from the plant extract, acting as capping agents around the AuNPs.

XRD spectra: The crystalline structure and average crystalline size of neem fruit pulp extracted mediated AuNPs were studied through XRD technique. Fig. 6 shows the XRD pattern of NFPE-AuNPs. The diffraction peaks at 2θ values of 38.265º, 44.418º, 64.697º and 77.663º correspond to the (111), (200), (220) and (311) planes of the face-centred cubic (FCC) structure of the synthesized AuNPs, according to JCPDS card no: 04-0784. These values are consistent with those reported for nano gold colloids in the literature [38]. Additionally, the XRD patterns show no peaks related to impurities and no significant peak shifts are observed indicating the purity of the synthesized gold nanoparticles. To calculate the average crystallite size, the Scherrer's equation was employed:

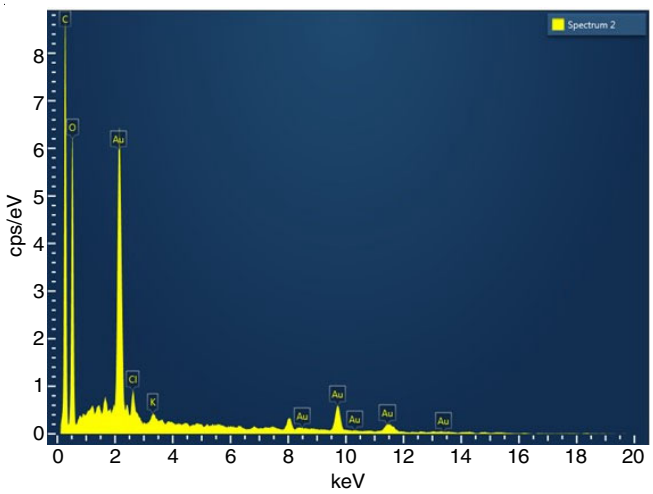

Fig. 5 EDX spectrum of AuNPs

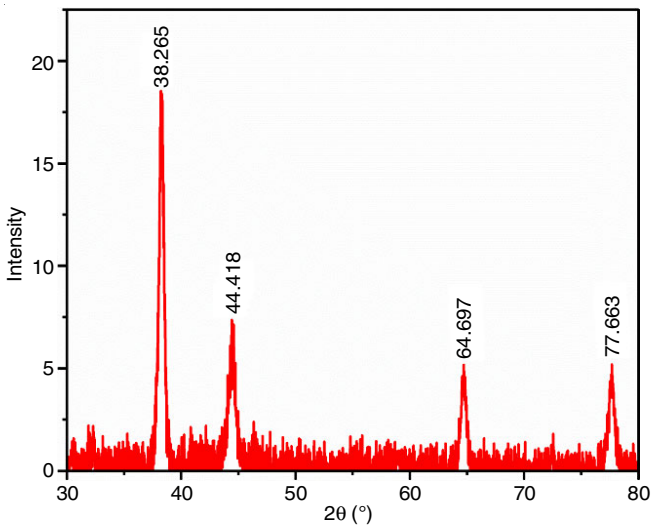

Fig. 6. XRD spectrum of AuNPs. The characteristic peak for gold (111) was found at 2θ = 38.265

$$D = \frac{0.94\lambda}{\beta\cos\theta}$$

where D represents the average crystallite size in nanometres, λ is the X-ray wavelength, β is the full width at half maximum and θ is the Bragg angle (Table-1) [39]. Based on this equation, the average crystallite size was found to be 17.4 nm.

TABLE-1
XRD DATA OF SYNTHESIZED AuNPs

Standard d-Spacing JCPDS No. 04-0784	Observed (2θ)	Observed d-spacing $d = \lambda/2 \sin\theta$	FWHM	d_{hkl}	D (nm)
38.117	38.265	2.35621	0.477	(111)	19.6
44.279	44.418	2.03789	o.672	(200)	12.7
64.428	64.697	1.43963	0.510	(220)	18.3
77.475	77.663	1.2284	0.597	(311)	19.0
			Average crystalline size		17.4

TEM and SAED studies: HRTEM analysis was used to examine the morphology such as shape and size of AuNPs synthesized using neem fruit pulp extract (Fig. 7a-b). The TEM observations revealed that gold nanoparticles exhibit a spherical shape with a smooth surface morphology. These nanoparticles, with diameters ranging from 10 nm to 15 nm, demonstrate a highly uniform distribution.

The crystalline arrangement of AuNPs was analyzed utilizing selected area electron diffraction (SAED) technique is shown in Fig. 7c. Bright circles in the pattern indicate the poly-

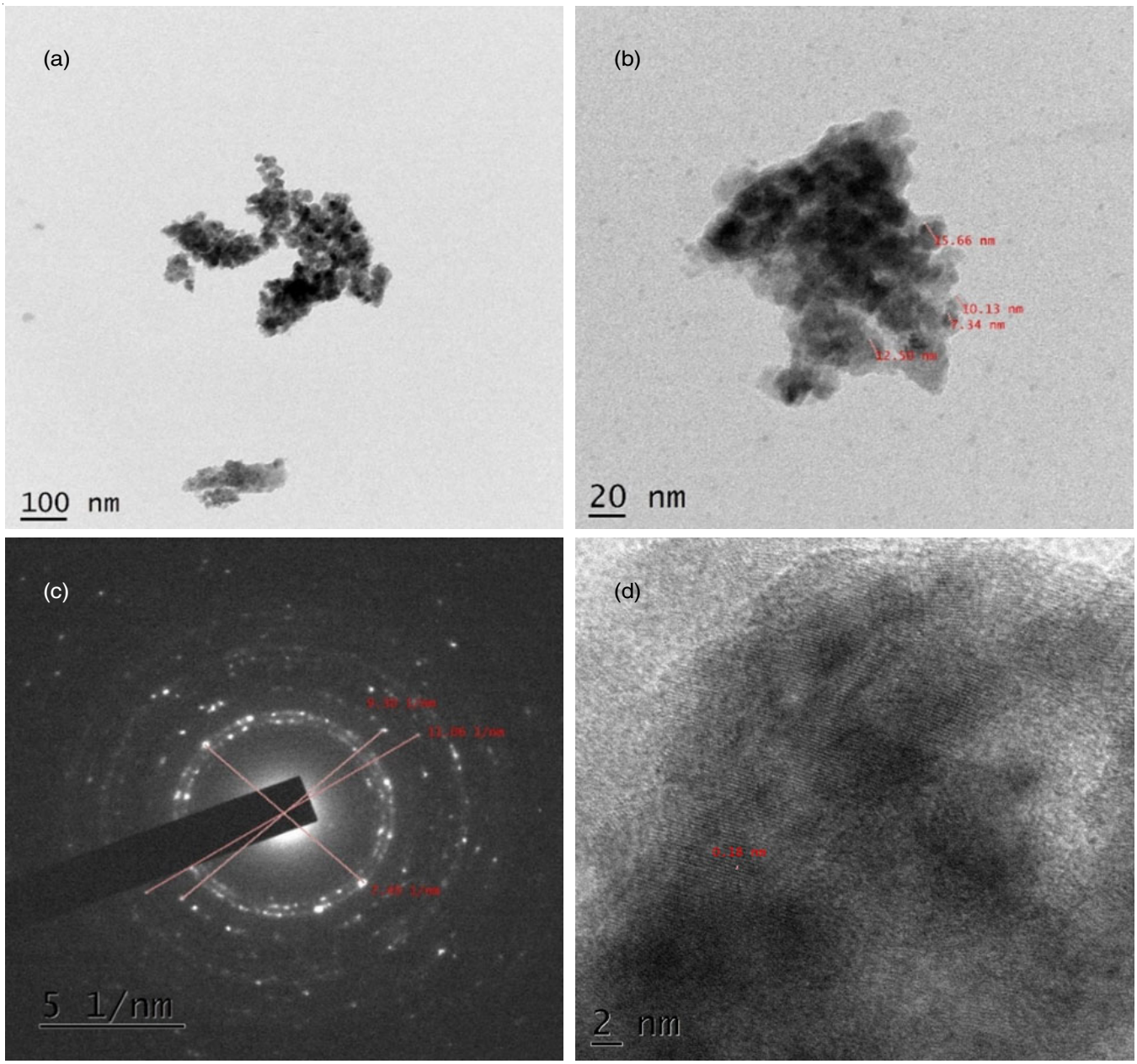

Fig. 7. (a-b) TEM images of NFE–AuNPs. It shows the presence of spherical nano particles with sizes ranging from 22-55 nm and (c-d) SAED patterns of the synthesized AuNPs

crystalline nature of the gold nanoparticles. The SAED results matched with the results obtained from XRD analysis and circular rings corresponding to (111), (200) and (220) planes in the SAED image signify the characteristic reflections of the face-centered cubic (FCC) crystalline structure of gold nanoparticles [40,41]. Furthermore, the crystalline structure of the AuNPs is made up of several crystalline lattices with a clearly defined inter-planer spacing of d = 0.18 nm (Fig. 7d). The results were similar to those from earlier reports [42].

Catalytic reduction of 4-nitrophenol: 4-Nitrophenol reduction reaction serves as a standard model for assessing the catalytic efficacy of synthesized NFPE-AuNPs, frequently presented in various research works on the catalytic abilities of green-synthesized AuNPs. After the addition of freshly prepared $NaBH_4$ solution, the 4-nitrophenol absorption peak undergoes a red shift from 318 to 400 nm, resulting in a colour change from light yellow to dark yellow due to the formation of 4-nitrophenolate ion [43]. The absorption peak at 400 nm is maintained for a long time (25 min) in absence of AuNPs (Fig. 8a), indicating that $NaBH_4$ cannot reduce the 4-nitrophenolate ion without a catalyst. In ambient conditions, AuNPs facilitate the rapid reduction of 4-nitrophenol to 4-aminophenol in the presence of $NaBH_4$ as displayed in Fig. 8b. A reduction of absorption peak of 4-nitrophenol at 400 nm over time, nearly disappearing after 15 min, this was followed by the appearance and gradual increase of peak at 300 nm, confirmed the formation of 4-aminophenol. Several studies have reported that the amount of nanocatalyst, the initial concentration of 4-nitrophenol and $NaBH_4$ are important factors that influence the catalytic reduction of 4-nitrophenol to 4-aminophenol by metal based nanoparticles [44,45]. Thus, when utilizing NFPE–AuNPs, the catalytic reduction proceeds finished within 15 min (97.30%). Table-2 shows the comparative data of the reaction time and size of the various AuNPs by green synthesis methodolgy utilized to reduce 4-nitrophenol.

Kinetic studies: The reaction rate, determined from ln A_0/A_t plotted against time (s), where A_0 and A_t represent the 4-nitrophenol absorbance at times 0 and t, respectively, exhibited a linear relationship with time, demonstrating excellent conformity to pseudo first-order kinetics with a correlation coefficient (R^2) of 0.98 and rate constant (k) is 0.11342 min^{-1} (Fig. 8c). In the presence of $NaBH_4$ and AuNPs, BH_4^- and 4-nitrophenol initially diffuse to the Au surface from the aqueous solution. The AuNPs serve as catalysts, facilitating electron transfer from BH_4^- to nitrophenol. Excess borohydride ions from $NaBH_4$ are adsorbed onto the AuNPs surface and then transfer a hydride to nitrophenol, leading to the reduction of 4-nitrophenolate to 4-aminophenol, attributed to the thermodynamically unstable hydrogen atoms interacting with 4-nitrophenolate during the hydrogenation process.

TABLE-2
COMPARATIVE DATA OF GREEN SYNTHESIZED AuNPs USED FOR THE REDUCTION OF 4-NITROPHENOL WITH THEIR SIZE AND REACTION TIME

Feedstock	Size (nm)	Reduction time (min)	Ref.
Citrus fruir extract	25	20	[47]
Caffeic acid	38	15	[48]
Mimusops eleugi	9-14	5-8	[49]
Sterculia acuminta	26.5	36	[50]
Caffca arabica	28	38	[46]

Catalytic reduction of methylene blue dye: Fig. 9a represents the spectrum of a solution containing $NaBH_4$ and methylene blue in absence of catalyst. However, after 25 min, solution peak was degraded slightly. Based on these observations clearly indicated that either methylene blue dye is not reduced effectively by $NaBH_4$ without catalyst [51,52]. On the other hand, upon addition of NFPE–AuNPs, the methylene blue almost degraded and the solutions became colourless within 10 min (Fig. 9b). Table-3 shows the comparative studies of methylene blue degradation with AuNPs synthesized from different sources.

TABLE-3
GREEN SYNTHESIS OF AuNPs AND APPLICATIONS FOR METHYLENE BLUE B DEGRADATION IN PRESENCE OF $NaBH_4$

Plant source	Degradation of MB dye (%)	Time required for reduction of MB dye	Ref.
Salvia officinalis	100	34 min	[53]
Oil palm	98.3	24 h	[54]
Sanseveieria roxhurghiana	49.6	1 h	[55]
Myristica fragrana	100	10 min	[56]
Edible coconut oil	100	20 min	[57]

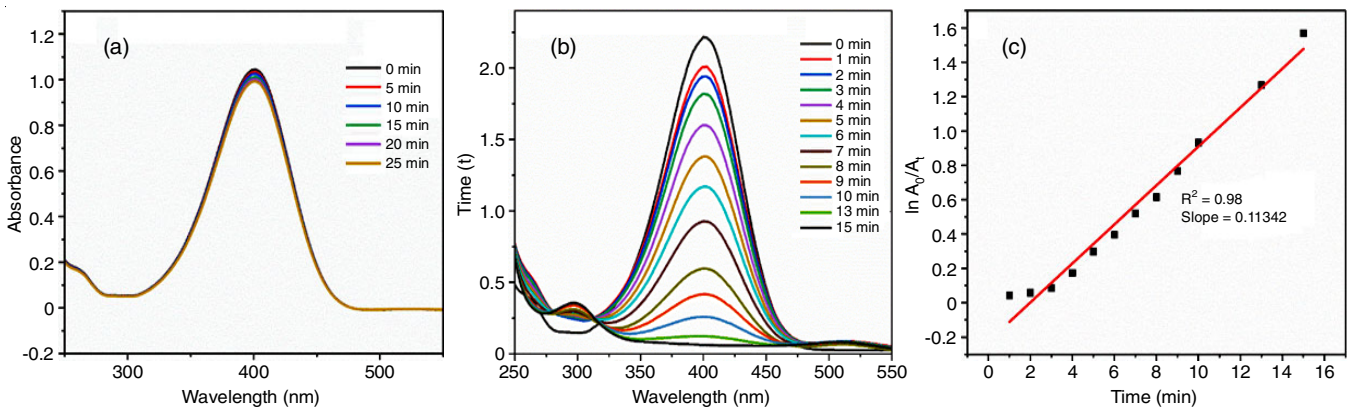

Fig. 8. Catalytic activity of AuNPs (a) time-dependent UV-vis absorption spectra for the reduction of 4-nitrophenol in the absence of AuNPs, (b) presence of AuNPs, (c) Plot of ln(A_0/A_t) *vs.* time (min) for the catalytic conversion of 4-nitrophenol

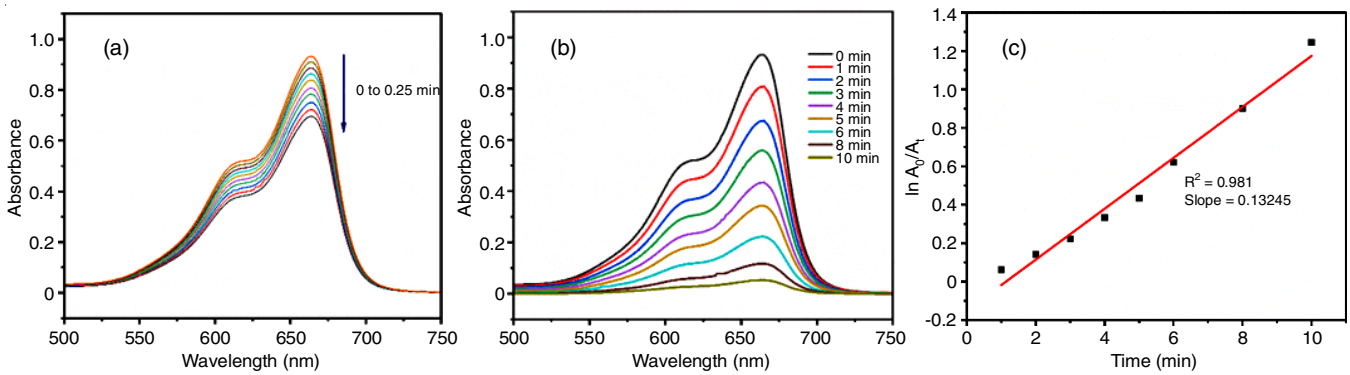

Fig. 9. (a) Reduction of methylene blue in the presence of $NaBH_4$ and absence of a catalyst, (b) Time-dependent UV-Vis spectra for the reduction of MB using AuNPs, (c) Plots of ln A_0/A_t *versus* time for the catalytic reduction of *p*-nitrophenol using AuNPs and $NaBH_4$

TABLE-4
ANTIOXIDANT ACTIVITY OF THE SYNTHESIZED AuNPs

Sample	10 µg/mL	25 µg/mL	50 µg/mL	75 µg/mL	100 µg/mL	IC_{50}
Au NPS	17.84	61.15	74.53	81.22	83.40	30.12
Ascorbic acid	40.89	65.98	81.04	87.36	93.68	7.42

Antioxidant activity: Recent studies have revealed that AuNPs, particularly those synthesized through green methods, possess significant antioxidant properties, attributed to the phytochemicals adhering to their surface [23]. The DPPH radical scavenging assay revealed that AuNPs effectively interacted with free oxygen radicals exhibiting the antioxidant properties [58]. In the concentration range of 10-100 µg/mL, green-synthesized AuNPs demonstrated inhibition percentages ranging from 17.84% to 83.4%, with an IC_{50} value of 30.12 µg/mL for DPPH activity. A remarkable 83% radical scavenging activity was observed with 100 µg/mL AuNPs. The antioxidant activity exhibited a dose-dependent pattern, with increasing nanoparticle concentration leading to higher % inhibition (Table-4).

Conclusion

An easy, eco-friendly and cost-effective method to synthesize biocompatible AuNPs using neem fruit pulp extract as a reducing and stabilizing agent is reported. The synthesized NFPE-AuNPs were examined through UV-vis, XRD, FTIR, EDX, DLS and TEM techniques. The synthesized AuNPs were spherical in shape and averaged 20 nm in size. They showed significant antioxidant properties and high catalytic efficiency in the reduction of 4-nitrophenol to 4-aminophenol and degradation of methylene blue dye.

ACKNOWLEDGEMENTS

The authors are thankful to DST-SAIF Cochin, India for providing the facilities of EDS, TEM and XRD analysis.

CONFLICT OF INTEREST

The authors declare that there is no conflict of interests regarding the publication of this article.

REFERENCES

1. M. Nasrollahzadeh, S.M. Sajadi, M. Sajjadi and Z. Issaabadi, An Introduction to Nanotechnology, in: Interface Science and Technology, Elsevier, Chap. 1, pp. 1–27 (2019); https://doi.org/10.1016/B978-0-12-813586-0.00001-8
2. E.J. Garboczi, Concrete Nanoscience and Nanotechnology: Definitions and Applications, In: Nanotechnology in Construction 3, Berlin, Heidelberg, Springer Berlin Heidelberg, pp. 81–88 (2009).
3. M. Ahmeda, N. Ahmida and A. Ahmeida, *Libyan Int. Med. Univ. J.* , **2**, 12 (2017); https://doi.org/10.21502/limuj.003.02.2017
4. S. H. Lee and B.-H. Jun, *Int. J. Mol. Sci.*, **20**, 865 (2019); https://doi.org/10.3390/ijms20040865
5. I. Hammami, N.M. Alabdallah, A. Al-Jomaa and M. Kamoun, *J. King Saud Univ. Sci.*, **33**, 101560 (2021); https://doi.org/10.1016/j.jksus.2021.101560
6. I. Saldan, Y. Semenyuk, I. Marchuk and O. Reshetnyak, *J. Mater. Sci*, **50**, 2337 (2015); https://doi.org/10.1007/s10853-014-8802-2
7. A.A. Hernández-Hernández, G. Aguirre-Álvarez, R. Cariño-Cortés, L.H. Mendoza-Huizar and R. Jiménez-Alvarado, *Chem. Papers*, **74**, 3809 (2020); https://doi.org/10.1007/s11696-020-01229-8
8. A. Kolodziejczak-Radzimska and T. Jesionowski, *Materials*, **7**, 2833 (2014); https://doi.org/10.3390/ma7042833
9. J. Wang, Z. Wang, W. Wang, Y. Wang, X. Hu, J. Liu, X. Gong, W. Miao, L. Ding, X. Li and J. Tang, *Nanoscale*, **14**, 6709 (2022); https://doi.org/10.1039/D1NR08349J
10. T. S. Sreeprasad and T. Pradeep, Noble Metal Nanoparticles, in Springer Handbook of Nanomaterials, Berlin, Heidelberg, Springer Berlin Heidelberg, pp. 303–388 (2013); https://doi.org/10.1007/978-3-642-20595-8_9
11. M. Rai, A.P. Ingle, S. Birla, A. Yadav and C.A. Dos Santos, *Crit. Rev. Microbiol.*, **42**, 696 (2015); https://doi.org/10.3109/1040841X.2015.1018131
12. V. Pareek, A. Bhargava, R. Gupta, N. Jain and J. Panwar, *Adv. Sci. Eng. Med.*, **9**, 527 (2017); https://doi.org/10.1166/asem.2017.2027
13. E.E. Elemike, D.C. Onwudiwe, L. Wei, L. Chaogang and Z. Zhiwei, *Solar Energy Mater. Solar Cells*, **201**, 110106 (2019); https://doi.org/10.1016/j.solmat.2019.110106
14. T. Pradeep and Anshup, *Thin Solid Films*, **517**, 6441 (2009); https://doi.org/10.1016/j.tsf.2009.03.195
15. R.R. Arvizo, S. Bhattacharyya, R.A. Kudgus, K. Giri, R. Bhattacharya and P. Mukherjee, *Chem. Soc. Rev.*, **41**, 2943 (2012); https://doi.org/10.1039/c2cs15355f
16. G. Doria, J. Conde, B. Veigas, L. Giestas, C. Almeida, M. Assunção, J. Rosa and P. V. Baptista, *Sensors*, **12**, 1657 (2012); https://doi.org/10.3390/s120201657

17. P.G. Jamkhande, N.W. Ghule, A.H. Bamer and M.G. Kalaskar, *J. Drug Deliv. Sci. Technol.*, **53**, 101174 (2019); https://doi.org/10.1016/j.jddst.2019.101174
18. E. Jiménez, K. Abderrafi, R. Abargues, J.L. Valdés and J.P. Martínez-Pastor, *Langmuir*, **26**, 7458 (2010); https://doi.org/10.1021/la904179x
19. S.A.M. Ealia and M.P. Saravanakumar, *IOP Conf. Ser. Mater. Sci. Eng.*, **263**, 032019 (2017); https://doi.org/10.1088/1757-899X/263/3/032019
20. S. Menon, S. Rajeshkumar and S.V. Kumar, *Resour.-Effic. Technol.*, **3**, 516 (2017); https://doi.org/10.1016/j.reffit.2017.08.002
21. K. X. Lee, K. Shameli, Y. P. Yew, S.-Y. Teow, H. Jahangirian, R. Rafiee-Moghaddam and T. Webster, *Int. J. Nanomedicine*, **15**, 275 (2020); https://doi.org/10.2147/IJN.S233789
22. M. Noruzi, D. Zare, K. Khoshnevisan and D. Davoodi, *Spectrochim. Acta A Mol. Biomol. Spectrosc.*, **79**, 1461 (2011); https://doi.org/10.1016/j.saa.2011.05.001
23. Y. Ngungeni, J.A. Aboyewa, K.L. Moabelo, N.R.S. Sibuyi, S. Meyer, M.O. Onani, M. Meyer and A.M. Madiehe, *ACS Omega*, **8**, 26088 (2023); https://doi.org/10.1021/acsomega.3c02260
24. M. Montazer and T. Harifi, Nanofinishing: Fundamental principles, In: Nanofinishing of Textile Materials, Elsevier, pp. 19–34 (2018); https://doi.org/10.1016/B978-0-08-101214-7.00002-9
25. Kh. Brainina, N. Stozhko, M. Bukharinova and E. Vikulova, *Phys. Sci. Rev.*, **3** (2018); https://doi.org/10.1515/psr-2018-8050
26. C.-S. Yeh, F.-Y. Cheng and C.-C. Huang, From Bioimaging to Biosensors: Noble Metal Nanoparticles in Biodetection, Jenny Stanford Publishing, edn. 1 (2012).
27. P.B. Santhosh, J. Genova and H. Chamati, *Chemistry*, **4**, 345 (2022); https://doi.org/10.3390/chemistry4020026
28. M. Hassanisaadi, G.H.S. Bonjar, A. Rahdar, S. Pandey, A. Hosseinipour and R. Abdolshahi, *Nanomaterials*, **11**, 2033 (2021); https://doi.org/10.3390/nano11082033
29. A.B. Babu, K.D. Bhavani Anagani and P. Sravanthi, *Asian J. Chem.*, **35**, 739 (2023); https://doi.org/10.14233/ajchem.2023.26988
30. J. K. Patra, Y. Kwon and K.-H. Baek, *Adv. Powder Technol.*, **27**, 2204 (2016); https://doi.org/10.1016/j.apt.2016.08.005
31. M.V. Sujitha and S. Kannan, *Spectrochim. Acta A Mol. Biomol. Spectrosc.*, **102**, 15 (2013); https://doi.org/10.1016/j.saa.2012.09.042
32. J.R. Nakkala, R. Mata and S.R. Sadras, *Process Safety Environ. Prot.*, **100**, 288 (2016); https://doi.org/10.1016/j.psep.2016.02.007
33. S.B. Kedare and R.P. Singh, *J. Food Sci. Technol.*, **48**, 412 (2011); https://doi.org/10.1007/s13197-011-0251-1
34. M. Hosny, M. Fawzy, A.M. Abdelfatah, E.E. Fawzy and A.S. Eltaweil, *Adv. Powder Technol.*, **32**, 3220 (2021); https://doi.org/10.1016/j.apt.2021.07.008
35. K. Arunachalam, S. Annamalai and S. Hari, *Int. J. Nanomedicine*, **2013**, 1307 (2013); https://doi.org/10.2147/IJN.S36670
36. S. Vanaraj, J. Jabastin, S. Sathiskumar and K. Preethi, *J. Clust. Sci.*, **28**, 227 (2017); https://doi.org/10.1007/s10876-016-1081-0
37. N.K.R. Bogireddy, U. Pal, L.M. Gomez and V. Agarwal, *RSC Adv*, **8**, 24819 (2018); https://doi.org/10.1039/C8RA04332A
38. S. Rajeshkumar, *J. Genetic Eng. Biotechnol.*, **14**, 195 (2016); https://doi.org/10.1016/j.jgeb.2016.05.007
39. C. Jayaseelan, R. Ramkumar, A.A. Rahuman and P. Perumal, *Ind. Crops Prod.*, **45**, 423 (2013); https://doi.org/10.1016/j.indcrop.2012.12.019
40. X. Yin, S. Chen and A. Wu, *Micro Nano Lett.*, **5**, 270 (2010); https://doi.org/10.1049/mnl.2010.0117
41. S. Gurunathan, J. Han, J. H. Park and J.-H. Kim, *Nanoscale Res. Lett.*, **9**, 248 (2014); https://doi.org/10.1186/1556-276X-9-248
42. M. Hamelian, S. Hemmati, K. Varmira and H. Veisi, *J. Taiwan Inst. Chem. Eng.*, **93**, 21 (2018); https://doi.org/10.1016/j.jtice.2018.07.018
43. N. Berahim, W.J. Basirun, B.F. Leo and M.R. Johan, *Catalysts*, **8**, 412 (2018); https://doi.org/10.3390/catal8100412
44. A.M. Madiehe, K.L. Moabelo, K. Modise, N.R. Sibuyi, S. Meyer, A. Dube, M.O. Onani and M. Meyer, *Nanomater. Nanotechnol.*, **12**, 1 (2022); https://doi.org/10.1177/18479804221108254
45. M.H. Oueslati, L. Ben Tahar and A.H. Harrath, *Green Chem. Lett. Rev.*, **13**, 18 (2020); https://doi.org/10.1080/17518253.2019.1711202
46. Y.R. Mejía and N.K. Reddy Bogireddy, *RSC Adv.*, **12**, 18661 (2022); https://doi.org/10.1039/D2RA02663E
47. J. Yu, D. Xu, H.N. Guan, C. Wang, L.K. Huang and D.F. Chi, *Mater. Lett.*, **166**, 110 (2016); https://doi.org/10.1016/j.matlet.2015.12.031
48. Z. Gao, R. Su, R. Huang, W. Qi and Z. He, *Nanoscale Res. Lett.*, **9**, 404 (2014); https://doi.org/10.1186/1556-276X-9-404
49. R. Majumdar, B.G. Bag and P. Ghosh, *Appl. Nanosci.*, **6**, 521 (2016); https://doi.org/10.1007/s13204-015-0454-2
50. N.K.R. Bogireddy, K.K. Hoskote Anand and B.K. Mandal, *J. Mol. Liq.*, **211**, 868 (2015); https://doi.org/10.1016/j.molliq.2015.07.027
51. K. Mallick, M. Witcomb and M. Scurrell, *Mater. Chem. Phys.*, **97**, 283 (2006); https://doi.org/10.1016/j.matchemphys.2005.08.011
52. K.B. Narayanan, H.H.Park and S.S. Han, *Chemosphere*, **141**, 169 (2015); https://doi.org/10.1016/j.chemosphere.2015.06.101
53. M.H. Oueslati, L. Ben Tahar and A.H. Harrath, *Green Chem. Lett. Rev.*, **13**, 18 (2020); https://doi.org/10.1080/17518253.2019.1711202
54. M. Irfan, M. Moniruzzaman, T. Ahmad, O.Y. Osman, P.C. Mandal, S. Bhattacharjee and M. Hussain, *J. Environ. Chem. Eng.*, **6**, 5024 (2018); https://doi.org/10.1016/j.jece.2018.07.031
55. R. Mata, A. Bhaskaran and S.R. Sadras, *Particuology*, **24**, 78 (2016); https://doi.org/10.1016/j.partic.2014.12.014
56. A. Ahmad, Y. Wei, F. Syed, M. Imran, Z.U.H. Khan, K. Tahir, A.U. Khan, M. Raza, Q. Khan and Q. Yuan, *RSC Adv.*, **5**, 99364 (2015); https://doi.org/10.1039/C5RA20096B
57. M. Meena Kumari and D. Philip, *Spectrochim. Acta A Mol. Biomol. Spectrosc.*, **111**, 154 (2013); https://doi.org/10.1016/j.saa.2013.03.076
58. S. Pu, J. Li, L. Sun, L. Zhong and Q. Ma, *Carbohydr. Polym.*, **211**, 161 (2019); https://doi.org/10.1016/j.carbpol.2019.02.007